CONTRAVARIANT AND COVARIANT POLYMER DUMBBELLS IN NON-AFFINE VISCOELASTIC TURBULENCE

Kiyosi Horiuti, Shohei Takeu
Department of Mechano-Aerospace Engineering, Tokyo Institute of Technology, Tokyo, Japan

Abstract
We carry out numerical study to reveal the mechanism of drag reduction (DR) in polymer-diluted flows. The polymer chains are modeled as elastic dumbbells. Primary purpose of this study is to elucidate the effect of introduction of non-affinity in the motion of dumbbells on DR. We consider the cases in which their motions do not precisely correspond to macroscopically-imposed deformation. We conduct analysis by connecting a macroscopic description for the Newtonian turbulent flow whose evolution is pursued using DNS to the mesoscopic description of an ensemble of dumbbells which are advected using the Brownian dynamics simulation (BDS) in forced homogeneous isotropic turbulence. The polymer stresses incurred by the dumbbells are fed back into the Navier-Stokes equation. Compared with the complete affine case ($\alpha = 0.0$), more drastic DR is achieved when non-affinity is maximum ($\alpha = 1.0$). When $\alpha = 0.0$, the connector vector of dumbbell is convected as a contravariant vector representing material line element and elasticity is caused on the tubular structures. When $\alpha = 1.0$, the connector vector is convected as a covariant vector representing material surface element, and directs outward perpendicularly on the planar structures and exert an extra tension on vortex sheet, which leads to attenuation of energy cascade, causing larger DR.

GOVERNING EQUATIONS FOR MOTION OF THE DUMBBELLS AND BDS-DNS RESULTS

It is well known that addition of small amount of long-chain polymers into the turbulent flow in the Newtonian fluid causes significant drag reduction (referred to hereafter as DR) relative to the Newtonian flow under the same conditions [1]. In previous studies, occurrence of DR is shown by solving the Navier-Stokes equation coupled with the viscoelastic polymer models to account for the effect of adding polymers ([2] and references therein). One of theoretical concepts of DR is due to Lumley [1]. He proposed that randomly coiled polymer molecules stretch in regions of strong deformation, increasing the elongation viscosity of the solution. This in turn results in damping of small turbulent eddies and DR. De Gennes [3] considered that Lumley scheme may hold for (rigid) rods, and in the coil-stretch transition, stretched chains behave elastically and it leads to modifications of the turbulent cascade. It is generally assumed that the Newtonian fluid which surrounds the bead-spring configuration of the polymers moves affinely with an equivalent continuum [4]. It is interesting to note that more remarkable DR is achieved when the fluid is diluted with different additives, e.g., cationic surfactant [5]. In the mixtures of polymers and fibers, DR exceeds the sum of DR obtained using either additive alone [6]. In the fluid diluted with stretched polymer or rod, molecular motions may not precisely correspond to the macroscopic deformation. In Horiuti *et al.* [7], the Johnson-Segalman (JS) model [8] was adopted to introduce non-affinity into the polymer stress. In both forced homogeneous isotropic turbulence and pipe flow, DR exhibited non-monotonous dependence on the strength of non-affinity (slip parameter $\alpha, 0 \leq \alpha \leq 1$). DR was maximal when non-affinity is either minimum ($\alpha = 0.0$) or maximum ($\alpha = 1.0$) and almost no DR was obtained when $\alpha = 0.5$. Remarkable enhancement of DR was achieved when $\alpha = 1.0$ in both flows.

One of limitations of the DNS using the constitutive equation is that it is not possible to identify exact configuration, orientation and alignment of the dumbbells due to coarse graining of the polymer scale. To remedy this drawback, we adopt multi-scale BDS-DNS approach [9] in the present study. The position vectors of each bead of the $n-$th dumbbell are denoted by $\boldsymbol{x}_1{}^{(n)}$ and $\boldsymbol{x}_2{}^{(n)}$ ($n = 1, 2, \cdots N_t$, N_t is the total number of dumbbells). When complete affinity is assumed, the governing equation for motion of the end-to-end connector vector $\boldsymbol{R}^{(n)} = \boldsymbol{x}_1{}^{(n)} - \boldsymbol{x}_2{}^{(n)}$ is given by [9]

$$\frac{dR_i{}^{(n)}}{dt} = \{u_i(x_1{}^{(n)}) - u_i(x_2{}^{(n)})\} - \frac{1}{2\tau_s} \frac{R_i{}^{(n)}}{1 - (R_k{}^{(n)} R_k{}^{(n)}/L_{max}{}^2)} + \frac{r_{eq}}{\sqrt{2\tau_s}} \left((W_1{}^{(n)})_i - (W_2{}^{(n)})_i \right), \qquad (1)$$

where $u_i(x)$ denotes the velocity field of the solvent fluid, and the finitely extensible nonlinear elastic (FENE) model is applied to the elastic force. $(W_{1,2}{}^{(n)})_i$ is a random force representing the Brownian motion of particles, which obeys Gaussian statistics. L_{max} is the maximum length which the dumbbell can extend. τ_s is the relaxation time and r_{eq} the equilibrium length of the dumbbell. This equation is solved together with that for the center-of-mass vector (see Fig. 1) [9]. We introduce the non-affinity by allowing a slippage in the motion of polymer strand [7]. The velocity imposed at bead i, is given as $\boldsymbol{u}_i = \boldsymbol{u}_g + (\nabla \boldsymbol{u}_g) \cdot (\boldsymbol{R}_i - \boldsymbol{R}_g) - 2\alpha\{\boldsymbol{S}_t \cdot (\boldsymbol{R}_i - \boldsymbol{R}_g)\}$, where $\boldsymbol{u}_g$ denotes the velocity at the center and $\nabla \boldsymbol{u}_g$ is the velocity gradient tensor and $\boldsymbol{S}_t$ is the strain rate.

When $\alpha = 0.0$, Eq. (1) is analogous to the equation for evolution of a contravariant vector field associated with a material line element of the fluid. If we initialize $\boldsymbol{R}$ to be a vortex line, then they evolve as fluid line elements. The dumbbells concentrate along the vortex lines and elasticity arise primarily in the vortex tube-like regions. When $\alpha = 1.0$, Eq. (1) becomes analogous to the equation for material surface element with its vector area $\boldsymbol{S}$. $\boldsymbol{S}$ is a covariant vector of which a generator is the material line element on the surface normal to $\boldsymbol{S}$. Thereby, if we initialize $\boldsymbol{R}$ to be a area vector, $\boldsymbol{R}$ is

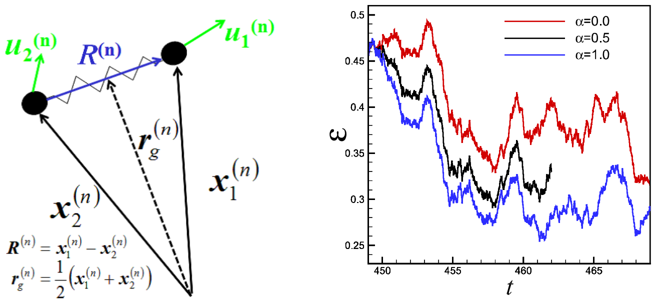

Figure 1. Left: Configurations of the two beads and connector vector.; Right: Temporal variations in the dissipation rate ε.

frozen into the fluid as the covariant vector and moves in association with the same surface. Elasticity arises in the vortex sheet region and $\boldsymbol{R}$ tends to become transversely aligned with the vorticity vector $\boldsymbol{\omega}$, whereas when $\alpha = 0.0$ $\boldsymbol{R}$ tends to become parallel to $\boldsymbol{\omega}$ [7].

We carried out DNS using 128^3 grid points, $\nu = 1/30, \tau_s = 1.5, Wi = 5.0, L_{max} = \eta(= 0.1), e_{eq} = L_{max}/50, N_t = 10^7$. Pseudospectral technique with a $3/2$-rule de-aliasing is used. The polymer stress tensor τ_{ij} due to the force acting on the fluid from the dispersed dumbbells which consists of the moments of the connector vectors are added to the Navier-Stokes equation. To attain the polymer stress whose amplitude is comparable to that of the stress obtained using the constitutive equation, prefactor ($\approx 10^5$) is multiplied to the original stress [9]. Figure 1 shows the temporal variations in ε. Small ε implies larger DR. When $\alpha = 0.0$ DR occurs, but DR in $\alpha = 1.0$ is more remarkable. $\alpha = 0.5$ denotes the case in which the dumbbells with $\alpha = 0.0$ and $\alpha = 1.0$ are evenly dispersed. Contrary to the same case in DNS with the JS model [7], DR intermediate between $\alpha = 0.0$ and 1.0 is obtained [6].

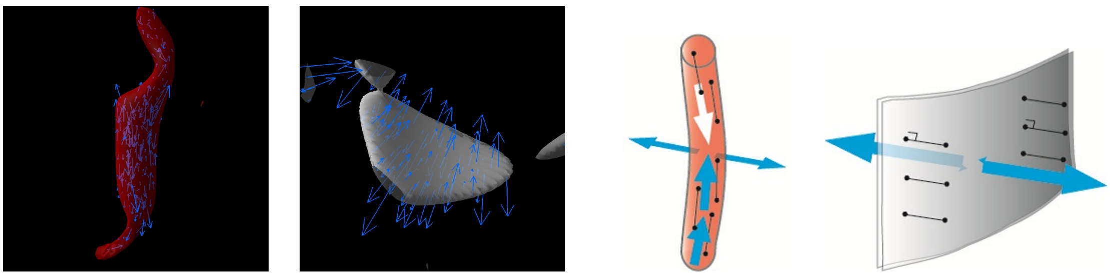

Figure 2. Left: Dumbbells (blue arrows) and isosurface of vortex tube ($\alpha = 0.0$) ; Middle left: Dumbbells and isosurface of vortex sheet ($\alpha = 1.0$); Middle right: Schematic of arrangement in $\alpha = 0.0$; Right: Schematic of arrangement in $\alpha = 1.0$.

Figure 2 shows the distributions of $\boldsymbol{R}$ in the cases of $\alpha = 0.0$ and 1.0. When $\alpha = 0.0$, the dumbbells align selectively in the axial direction of the tube (shown in red color), and the torque force due to polymer stress oppose to the vortex stretching and elongation of the tube is annihilated. When $\alpha = 1.0$, the dumbbells align preferentially in the direction normal to the surface of vortex sheets (shown in gray color). The polymer force reacts as the tensile force on the sheet and tends to pull back the sheet to the original form and stretching and thinning of the sheet is reduced as predicted in [7].

References

[1] J.L. Lumley: Drag reduction by additives. *Annual Rev. Fluid Mech.* **1**:367-384, 1969.

[2] K. Kim, R. J. Adrian, S. Balachandar and R. Sureshkumar: Dynamics of hairpin vortices and polymer-induced turbulent drag reduction, *Phys. Rev. Lett.* **100** 134504 2008.

[3] P.G. de Gennes: Towards a scaling theory of drag reduction. *Physica* **140A**:9-25, 1986.

[4] R.B. Bird, R.C. Armstrong, O. Hassanger: *Dynamics of polymeric liquids*. John Wiley and Sons Inc., 1987.

[5] J.L. Zakin, J. Myska, and Z. Chara: New limiting drag reduction and velocity profile asymptotes for nonpolymeric additives systems. *AIChE J.* **42**:3544, 1996.

[6] W. Lee, R. Vaseleski, and A. Metzner: Turbulent drag reduction in polymeric solutions containing suspended fibres, *AIChE J.* **20**:128, 1974.

[7] K. Horiuti, K. Matsumoto and K. Fujiwara: Remarkable drag reduction in non-affine viscoelastic turbulent flows, *Phys. Fluids* **25**: 015106, 2013.

[8] M.W. Johnson Jr. and D. Segalman: A model for viscoelastic fluid behavior which allows non-affine deformation. *J. Non-Newtonian Fluid Mech.* **2**:255-270, 1977.

[9] T. Watanabe, and T. Gotoh: Hybrid Eulerian Lagrangian simulations for polymer-turbulence interactions, *J. Fluid Mech.*: in press, 2013.